



# Optical coherence tomography: A pilot study of a new imaging technique for noninvasive examination of cervical tissue

Andrés F. Zuluaga, PhD,<sup>a,b</sup> Michele Follen, MD, PhD,<sup>c,d,f,\*</sup> Iouri Boiko, MD, PhD,<sup>g</sup>  
Anaís Malpica, MD,<sup>e</sup> Rebecca Richards-Kortum, PhD<sup>a</sup>

*Department of Biomedical Engineering, The University of Texas at Austin, Austin, TX<sup>a</sup>; InfraRedX, Boston, MA<sup>b</sup>; Biomedical Engineering Center,<sup>c</sup> Departments of Gynecologic Oncology,<sup>d</sup> Pathology,<sup>e</sup> The University of Texas MD Anderson Cancer Center, Departments of Gynecology, Obstetrics and Reproductive Sciences,<sup>f</sup> and Pathology, The University of Texas Health Science Center at Houston, Houston, TX<sup>g</sup>*

Received for publication November 25, 2003; revised October 7, 2004; accepted November 24, 2004

## KEY WORDS

Optical coherence tomography  
CIN  
SIL  
Cervical intraepithelial neoplasia  
Squamous intraepithelial neoplasia

**Objective:** Optical coherence tomography (OCT) is a novel noninvasive technique that can map subsurface tissue structure with a resolution of 10 to 20  $\mu\text{m}$ . The objective of this study was to determine whether an OCT imaging system could be used clinically in vivo to image and distinguish features of normal and abnormal cervical tissue.

**Study design:** Cervical OCT images and biopsy specimens were obtained from consenting volunteers. Images were analyzed quantitatively for intensity of backscattered light from the epithelia and for rates of signal decay of signal over the depth of epithelia (slope). Patients were stratified by menopausal status, and parameters were compared in normal and abnormal cervical samples, as diagnosed by routine histopathologic techniques.

**Results:** Average epithelial intensities were significantly stronger in the abnormal tissue than in the normal tissue of premenopausal women ( $P < .0024$ ), but were stronger in the normal tissue of postmenopausal women ( $P < .062$ ). No significant differences in signal decay rate were detected.

**Conclusion:** OCT images, which contain information about epithelial and stromal structure, can be clinically obtained. Image features of normal and abnormal cervical epithelium differ significantly.

© 2005 Elsevier Inc. All rights reserved.

Currently, the diagnosis of cervical cancer and its precursors requires histopathologic evaluation of colposcopy-directed biopsies. While the sensitivity associated

with colposcopy is high, the technique is expensive and typically requires that patients wait 2 weeks before necessary treatment can be scheduled. New techniques that provide increased sensitivity and specificity and can provide treatment instantaneously without the need for tissue removal could reduce both costs associated with the detection of cervical cancer and the loss of patients to follow-up.

Supported by NSF grant BES-9872829.

\* Reprint requests: Michele Follen, MD, PhD, UT-MD Anderson Cancer Center, Box 193, 1515 Holcombe Blvd, Houston, TX 77030-4009.

E-mail: [bcrain@mdanderson.org](mailto:bcrain@mdanderson.org); [mfollen@mdanderson.org](mailto:mfollen@mdanderson.org)

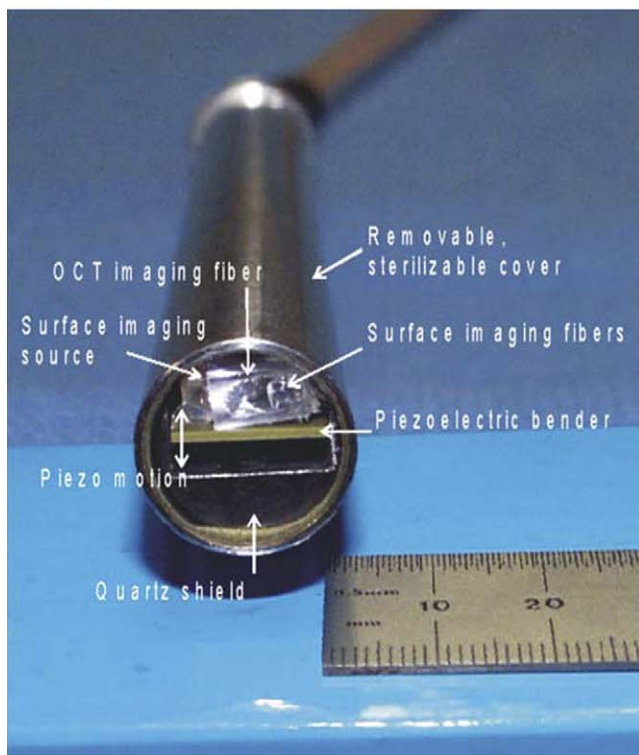


**Figure 1** Photograph of OCT system used in the clinical study and its probe.

A number of new imaging techniques that evaluate the cervical epithelium at the first patient visit are under investigation. Several optical techniques, such as elastic backscattering, and fluorescence and Raman spectroscopies, have been used to noninvasively probe tissue morphology and biochemical composition.<sup>1-6</sup> Optical

coherence tomography (OCT), another imaging technique, uses coherent light to form images of subsurface tissue structure noninvasively with 10 to 20  $\mu\text{m}$  resolution up to 1 mm in depth.<sup>7-10</sup> Beams of light are coherent when the phase difference between their waves is constant. Recently, *in vitro*<sup>11</sup> and *in vivo*<sup>12,13</sup> OCT imaging of cervical tissue illustrated that gross epithelial and stromal morphology can be imaged in near real time. However, the quantitative content of these images has not been explored in the literature. The purpose of this study was to examine whether simple quantitative analysis of OCT images obtained *in vivo* could distinguish histologically normal and abnormal cervical tissue samples.

OCT is an optical imaging technique capable of building two-dimensional reflectance maps from small signals within a scattering medium. OCT has been very successful in imaging the transparent tissue in the eye,<sup>8</sup> and has recently been used to image highly scattering media such as tissue and skin.<sup>9-13</sup> OCT is very similar to ultrasound, measuring the intensity of reflected light rather than sound waves. Because time of flight data for light cannot be measured directly, interferometric techniques are used. Small fluctuations in the refractive index of tissue, such as the boundary between the nucleus and cytoplasm, produce reflections which can be detected by OCT.

## Material and methods

### OCT system

The clinical system used to obtain OCT images of cervical tissue (Figure 1) has been previously described.<sup>14</sup> Briefly, it consists of a superluminescent diode emitting at 855 nm (Superlum Diodes, Ltd, Moscow, Russia), coupled into a fiber-optic Michelson interferometer (Gould Electronics, Inc, Millersville, Md). The distal end of the fiber-optic probe delivers light to the sample, and collects and records the depth-resolved intensity of the reflected light. The illumination power of the system was 500  $\mu\text{W}$ . Image acquisition required 3.5 seconds.

### Study population

OCT images of human cervical tissue were obtained from volunteers at 3 colposcopy clinics in Houston. Informed consent was obtained from all patients under a clinical protocol reviewed, and approved by the Institutional Review Boards at The University of Texas at Austin, The University of Texas MD Anderson Cancer Center, The University of Texas Health Science Center at Houston, and the Harris County Health District. Patients visiting the colposcopy clinics were

eligible to participate in the study if they were at least 18 years old and were not pregnant. All patients were referred to the clinics with abnormal Pap smears ranging from atypical squamous cells of undetermined significance (ASCUS) to cervical intraepithelial neoplasia (CIN).

### Measurements and biopsies

One OCT measurement was obtained from each quadrant of the cervix from each patient after speculum insertion and colposcopic examination. All measurements were made by one gynecologist. After OCT measurements were obtained, cotton balls soaked in acetic acid were placed in contact with the cervix for approximately 3 minutes in preparation for a second colposcopy. After a second colposcopic inspection, the areas measured by OCT were examined, and the clinical impressions recorded. Tissue samples were obtained from these same areas, either by traditional biopsy methods (a punch biopsy, 2 patients), or from a loop electrosurgical excision procedure (LEEP, 11 patients). The tissue samples were submitted for routine histopathologic examination. In the LEEP specimens, a stitch was sewn at the 12 o'clock position, and the endo- and ectocervical margins were inked to aid with tissue orientation during histopathologic examination. All histopathologic slides were read by 2 pathologists blinded to the results of OCT imaging. Samples were classified using standard histopathologic criteria. Samples with no conclusive diagnosis were discarded from the analysis.

### OCT imaging

Images were printed using a gray-scale map, and examined by 2 investigators blinded to the histopathologic results. Image intensity was reported in a logarithmic scale (dB units). Higher backreflection was indicated by less negative values, which corresponded to whiter shades on the image. Typically, OCT images show a layered structure; for each image, the extent of the uppermost layer was marked. A custom written program then calculated the average intensity of back-scattered light and the signal decay rate of the uppermost layer identified in each image. The signal decay rate was calculated by subtracting the average intensity of the bottom 5  $\mu\text{m}$  of the region of interest from the average intensity of the uppermost 5  $\mu\text{m}$  and dividing the result by the layer's thickness. A more negative rate corresponded to more rapid signal decay with depth. Samples with positive rates were excluded from the analysis because they did not make physical sense, and were likely the result of errors in epithelial layer segmentation.

**Table I** Histologic diagnoses of measured sites from all volunteers

Volunteer number	Biopsy/ LEEP	Site number	Histologic diagnosis
1	Biopsy	1	No biopsy
		2	Normal
		3	Normal
2	Biopsy	1	HPV
		2	Normal
		3	No biopsy
3		(3 OCT meas.)	No histology
4		(4 OCT meas.)	No histology
5	LEEP	1	Normal
		2	Normal
		3	CIN3
		4	Normal
6	LEEP	1	No OCT
		2	CIN2
		3	HPV
		4	Normal
8	LEEP	1	Normal
		2	Normal
		3	Normal
		4	Normal
9	LEEP	1	CIN3
		2	HPV
		3	Normal
		4	Normal
10	LEEP	(4 samples)	Inadequate histology
		1	Normal
		2	HPV
		3	Normal
12	LEEP	4	CIN1
		1	Normal
		2	Normal
		3	Normal
13	LEEP	4	Normal
		1	CIN3
		2	CIN3
		3	CIN3
14	LEEP	4	CIN3
		1	Normal
		2	Normal
		3	Normal
15	LEEP	4	Normal
		1	CIN3
		2	CIN2
		3	CIN3
16	LEEP	4	CIN3
		1	No epithelium in OCT
		2	Inadequate histology
		3	Normal
		4	HPV

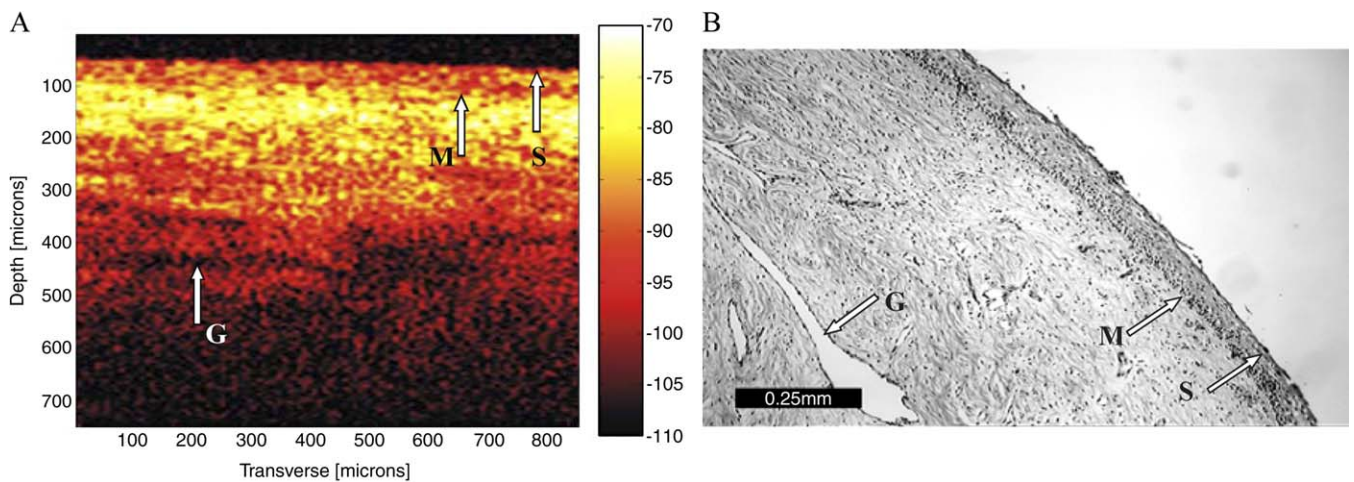


**Figure 2** Comparison between a typical OCT image (A) and a histology slide stained with hematoxylin and eosin (B). Visible in the OCT image and the biopsy sample are the tissue surface (S), the basement membrane (M) and glands in the connective tissue (G).

### Sample segregation

After image analysis was completed, the tissue samples measured by OCT were segregated as normal or abnormal based on histopathologic diagnoses; abnormal samples included koilocytosis and all grades of CIN and cervical cancer. Samples were also segregated according to the menopausal status of the patients from whom they came (pre- and postmenopausal).

### Statistical analysis

Although some images came from the same patient, each was treated as an independent sample. We used the nonparametric Wilcoxon W test to compare the measured parameters because of the small data set. The chi-square approximation for the distribution of the W deviate was used. For each comparison, the null hypothesis was that the means were equal in normal and abnormal samples. The alternate hypothesis was that the means were different. The null hypothesis was rejected if the probability of it being true was less than 10% ( $P < .100$ ) because the sample size was so small.

### Results

The 16 study participants ranged in age from 18 to 62 years, with a median of age of 37 years (Table I). One patient was of Asian ethnicity, 6 were black, 8 were Caucasian, and 1 was Hispanic. Eight of the volunteers smoked, and 8 did not. From the 16 patients participating in the study, there were 57 OCT measurements made. From these 57 sites, histopathologic interpretations were successfully made from 42 of the 57 sites. Instrument malfunction accounted for 1 patient not being sampled. Two patients refused biopsies after consenting to study. In 2 additional cases, the epithelium

**Table II** Number of sites in each diagnostic category and for each menopausal status

Histologic diagnosis	Menopausal status	
	Premenopausal	Postmenopausal
Normal	14	11
HPV	5	0
CIN1	1	0
CIN2	2	0
CIN3	4	5
Total normal	14	11
Total abnormal	12	5
Total	26	16

was detached from the stroma in the specimens, and the OCT image could not be correlated with the pathology.

Figure 2 shows a typical OCT image and the corresponding histology slide stained with H&E. The OCT image measures 750 by 850  $\mu\text{m}$  (depth by width); the scale bar in the histology slide measures 250  $\mu\text{m}$ . The strength of backscatter is encoded as a logarithmic gray scale. White corresponds to the highest backscatter, and black to the lowest. The topmost, dark band in the OCT image corresponds to the shield of the fiber-optic probe. The shield is transparent and so no light is reflected from it. The next observable feature (with increasing depth) in the OCT image is a sharp signal increase that corresponds to the tissue surface (S). The signal then fades, becoming darker as depth increases until the basement membrane (M) is reached. This is marked by another sharp signal increase. The signal then decays again with increasing depth until the noise level is reached. Apart from the 2-layered structure of the cervix, other features such as glandular structures in the connective tissue (G) are sometimes observed.

Table II shows the number of sites available for further analysis by diagnostic category and menopausal

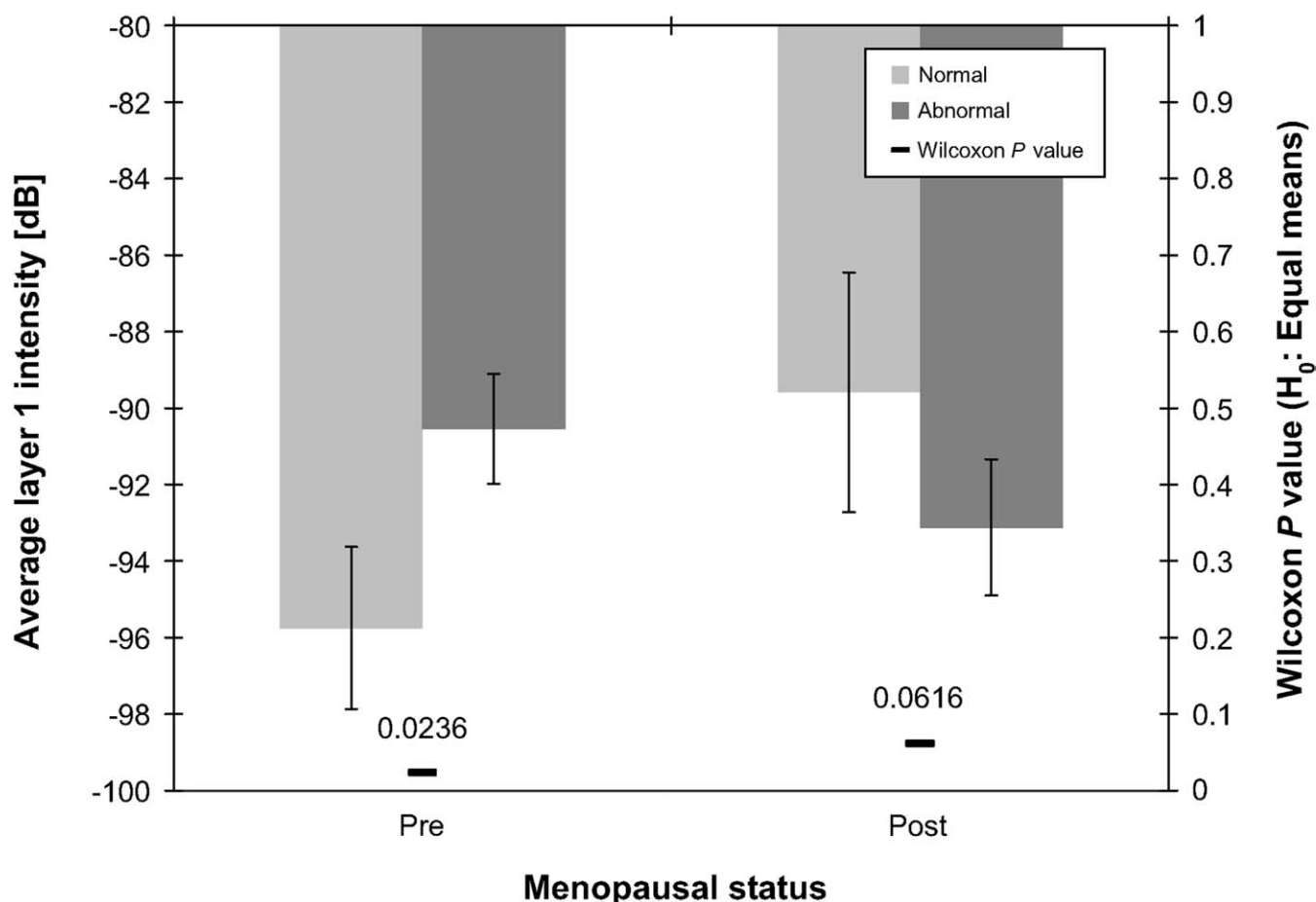


**Figure 3** Average epithelial backscattering intensity for normal and abnormal cervical specimens in pre- and postmenopausal women. Error bars mark the 90% CIs. The Wilcoxon  $P$  values  $< .1$  are reported as a labeled horizontal dash at the bottom of the figure (scale on the right vertical axis).

status. Average image intensities, and 90% Student  $t$  confidence intervals for the image parameters were obtained from the images collected in vivo, as segregated by normal and abnormal histologic samples and by patients' menopausal status (Figure 3). The average epithelial intensities for premenopausal women were significantly stronger in the samples of abnormal epithelium than in samples of normal epithelium ( $P < .024$ ). In postmenopausal women, the opposite trend was observed, with the average epithelial intensities stronger in normal epithelium than in abnormal epithelium, but the difference was not as significant ( $P < .062$ ). The average signal decay rates in the premenopausal group were not statistically different in the normal and abnormal samples. There were insufficient samples to compare these values in the postmenopausal group.

### Comment

We showed that an OCT system can be used clinically in vivo to produce images of cervical tissue. The average

epithelial intensities on OCT images of histologically normal and abnormal cervical tissues were statistically different. While very preliminary observations, we saw that by using OCT in real time we could easily distinguish the nuclei of cells from normal versus CIN 3 lesions. This was a small pilot study. Larger studies designed to look at normal patients and at abnormal patients, both with biopsy confirmation, need to be designed to confirm that OCT will have the sensitivity and specificity that merit further development.

OCT imaging illustrates gross morphologic features throughout and beneath the cervical epithelium. Quantitative features of the images differ in samples from patients with or without dysplasia and from pre- and postmenopausal patients. The average epithelial brightness increases as dysplasia develops. This increase in backscattering is consistent with the increase in scattering cross-section (a medium's ability to scatter light) of cells as nuclear size increases.<sup>15,16</sup> More scattering has also been reported in abnormal samples than in normal samples by Sergeev et al,<sup>12</sup> but the levels have not been quantified. In our study, we also found that

backscattering of light from the normal epithelium was more intense in postmenopausal women than in premenopausal women. This is consistent with an expected increase in scattering cross-section induced by the increase in nuclear to cytoplasmic ratio that occurs with menopause. Because the changes that occur in the menopause mimic those in dysplasia, a larger study including more pre- and postmenopausal patients must be performed to validate and test an algorithm that differentiates between histologically normal and abnormal samples.

In conclusion, this study showed that simple quantitative analysis of images obtained with a clinically viable OCT system can be used to noninvasively assess normal and abnormal cervical tissue *in vivo*. The use of noninvasive OCT imaging could have broad applications for screening, detection, and surgical-margin planning, including allowing surgeons to identify margins *in vivo* without obtaining frozen sections. Because they are easy to use and do not require provider education, OCT imaging systems can potentially be used by less-trained individuals in both screening and diagnostic settings. OCT is one of many promising optical techniques for the early detection of cancers and pre-cancers. These techniques may soon change the way medicine is practiced both in developed and developing countries.

## References

1. Ramanujam N, Mitchell MF, Mahadevan A, Richards-Kortum R. Fluorescence spectroscopy: a diagnostic tool for cervical intraepithelial neoplasia (CIN). *Gynecol Oncol* 1994;52:31-8.
2. Nishioka NS. Laser-induced fluorescence spectroscopy [review]. *Gastrointest Endosc Clin N Am* 1994;4:313-26.
3. Richards-Kortum R, Sevick-Muraca E. Quantitative optical spectroscopy for tissue diagnosis. *Annu Rev Phys Chem* 1996;47:555-606.
4. Bigio JJ, Mourant JR. Ultraviolet and visible spectroscopies for tissue diagnostics: fluorescence spectroscopy and elastic-scattering spectroscopy [review]. *Phys Med Biol* 1997;42:803-14.
5. Bohorfoush AG. Tissue spectroscopy for gastrointestinal diseases [review]. *Endoscopy* 1996;28:372-80.
6. Coppelson M, Pixley E, Reid B. *Colposcopy*. Springfield, IL: Charles C. Thomas Publisher; 1978.
7. Huang D, Swanson EA, Lin CP, Schuman JS, Stinson WG, Chang W, et al. Optical coherence tomography. *Science* 1991;254:1178.
8. Swanson EA, Izatt JA, Hee MR, Huang D, Lin CP, Schuman JS, et al. *In vivo* measurements of human retinal structure using optical coherence tomography. *Opt Lett* 1993;18:1864.
9. Izatt JA, Hee MR, Owen GA, Swanson EA, Fujimoto JG. Optical coherence microscopy in scattering media. *Opt Lett* 1994;19:590-2.
10. Izatt JA, Kulkarni MD, Wang H-W, Kobayashi K, Sivak MV. Optical coherence tomography and microscopy in gastrointestinal tissues. *IEEE J Select Topics Quantum Electron* 1996;4:1017-28.
11. Pitris C, Goodman A, Boppart S, Libus J, Fujimoto JG, Brezinski ME. High resolution imaging of gynecologic neoplasms using optical coherence tomography. *Obstet Gynecol* 1999;93:135-9.
12. Sergeev AM, Gelikonov VM, Gelikonov GV, Feldchtein FI, Kuranov RV, Gladkova ND, et al. *In-vivo* Endoscopic OCT Imaging of Precancer and Cancer States of Human Mucosa. *Optics Express* 1997;1:432-40.
13. Feldchtein FI, Gelikonov GV, Gelikonov VM, Kuranov RV, Sergeev AM, Gladkova ND, et al. Endoscopic applications of optical coherence tomography. *Optics Express* 1998;3:257-70.
14. Zuluaga AF. Development of a cervical probe for optical coherence imaging *in-vivo*. Department of electrical and computer engineering. Austin, TX: The University of Texas at Austin; 1998.
15. Dunn A, Richards-Kortum R. Three-dimensional computation of light scattering from cells. *IEEE J Select Topics Quantum Electronics* 1997;2:898-905.
16. Drezek RA, Dunn A, Richards-Kortum R. Finite difference time domain modeling and goniometric measurements of light scattering from cells. *Appl Opt* 1999;38:3651-61.